

Article

Spatiotemporal Analysis of Diurnal Temperature Range: Effect of Urbanization, Cloud Cover, Solar Radiation, and Precipitation

Andri Pyrgou ^{1,*}, Mattheos Santamouris ^{2,*} and Iro Livada ³

¹ Department of Civil Aviation, Pindarou 27 street, Nicosia 1429, Cyprus

² Faculty of Built Environment, University of New South Wales, Sydney 2052, Australia

³ Physics Department, National and Kapodistrian University of Athens, GR-15784 Athens, Greece

* Correspondence: a_pyrgou@hotmail.com (A.P.); m.santamouris@unsw.edu.au (M.S.)

Received: 5 May 2019; Accepted: 3 July 2019; Published: 6 July 2019



Abstract: High daily temperatures in the Mediterranean and Europe have been documented in observation and modeling studies. Long-term temperature data, from 1988 to 2017, from a suburban station and an urban station in Nicosia, Cyprus have been analyzed, and the diurnal temperature range (DTR) trend was investigated. The seasonal Mann–Kendall test revealed a decreasing DTR trend of -0.24 °C/decade at the urban station and -0.36 °C/decade at the suburban station, which were attributed to an increase in the daily minimum temperature. Variations in precipitation, longwave radiation, ultraviolet-A (UVA), ultraviolet-B (UVB), cloud cover, water vapor, and urbanization were used to assess their possible relationship with regional DTR. The clustering of daytime and night-time data showed a strong relationship between the DTR and observed cloud cover, net longwave radiation, and precipitation. Clouds associated with smaller shortwave and net longwave radiation reduce the DTR by decreasing the surface solar radiation, while atmospheric absolute humidity denotes an increased daytime surface evaporative cooling and higher absorption of the short and longwave radiation. The intra-cluster variation could be reduced, and the inter-cluster variance increased by the addition of other meteorological parameters and anthropogenic sources that affect DTR in order to develop a quantitative basis for assessing DTR variations.

Keywords: DTR; cluster; rainfall; water vapor; urban development; longwave radiation

Highlights

- Clustering analysis of meteorological parameters was used to characterize DTR variations
- DTR decreased over the years due to the large increase of minimum daily temperature
- Low DTR was associated with high net longwave radiation at night and low net longwave radiation during the daytime
- DTR was up to 4 °C higher during the warmer months
- High DTR was associated with high daytime net longwave radiation and low cloudiness

1. Introduction

The population in Europe (EU-28) reached 503 million according to Eurostat in 2011 [1], increasing by about 200 million people in a century. The increase of population over the past century combined with intensive urbanization and industrialization have led to a continuing increase of CO₂ emissions, local and global climate change, and an important increase in the ambient temperature [2].

Local climate change and urban heat island increase the ambient temperature in urban areas compared to the surrounding suburban and rural areas. Increased urban temperatures have a serious impact on the cooling energy consumption of buildings [3], peak electricity demand [4], and health [5].

The diurnal temperature range (DTR) is the difference between the daily maximum temperature and the minimum temperature, and may provide more information than the mean temperatures in the investigation of local and global climate change. Studies showed that surface warming is associated with larger increases in the daily minimum temperature rather than an increase in the maximum temperature over the past century [6–9]. DTR may be largely affected by the impacts of urbanization [7,10,11] and land-use changes [11,12]. Other parameters affecting DTR are cloud cover and precipitation [13,14]. Specifically, clouds may reduce the shortwave radiation reaching the surface, leading to a lower daily maximum temperature, and increase the minimum daily temperature by enhancing downward longwave radiation. Moreover, precipitation increases the level of soil moisture, enhances surface–air interactions that lead to larger evaporation, and results in a lower daily maximum temperature [13,14]. Dai et al. [13] showed that clouds, soil moisture, and precipitation can reduce the surface DTR by over 50% compared with clear sky days, and that atmospheric water vapor has the ability to increase both the minimum and maximum daily temperatures [13]. Additionally, atmospheric greenhouse gases and water vapor may promote larger downward longwave radiation and increase the minimum daily temperature.

Temperature trends have been explored in recent years, evaluating the effect of local and global climate change in urban and rural areas. Pastor et al. [15] have reported a consistent warming trend for the Mediterranean sea surface temperature (SST) with a mean total of 1.27 ± 0.12 °C for the 1982–2016 period [15], and in similar studies, a warming of 0.4 °C/decade for the period 1985–2006 [16,17]. Founda et al. [18] studied the annual mean air temperature in Athens, Greece and revealed an increase of 0.2 °C/decade for years 1970–2004 [18]. Wang et al. [11] for 559 stations across China found an increasing trend of 0.24 °C/decade for minimum temperature for the years 1961–1989; this was likely because of the impact of the greenhouse effect, which later increased at a rate above 0.37 °C/decade between 1990–2009 [11]. The global land surface DTR significantly decreased at a rate of -0.036 °C/decade over the 1901–2014 period according to Sun et al. [19]. Whan et al. [20] focused on the effect of soil moisture on extreme maximum temperatures in southern–central and southeastern Europe for years 1984–2013 and found a 2–4 °C increase under dry soil moisture conditions compared to wet conditions [20]. A DTR analysis in Spain for the years 1950–2011 revealed a high decreasing DTR trend (-0.11 °C to -0.29 °C per decade) for stations located by the Mediterranean Sea [21]. Price et al. [22] analyzed the long-term temperature data in Nicosia and Limassol in Cyprus for 1900–2000 showing a decrease of the DTR trend of -0.5 °C/100 years in the beginning of the century to -3.5 °C/100 years [22] by the end of the century, depending on the location. Seasonality was also examined in their study, showing a DTR trend of -1.4 °C/100 years and -5.3 °C/100 years for winter (DJF) and summer (JJA) respectively in Limassol and -0.1 °C/100 years and -0.9 °C/100 years for winter (DJF) and summer (JJA), respectively in Nicosia [22]. The two main possible causes of these DTR changes were related to the increased urbanization in Cyprus that leads to an enhanced urban heat island effect during night-time hours and to regional or global climate changes such as increased cloud cover, precipitation, and atmospheric aerosols [22].

Therefore, in this study, we quantify the magnitude of DTR trend in the capital of Cyprus, Nicosia and examine its yearly variations. The goal of this study is to improve understandings of how maximum and minimum daily temperatures and diurnal temperature range vary due to urbanization and regional or global climate changes of absolute humidity, net longwave radiation, and cloud cover. Moreover, we investigated the concurrent variations of ambient air temperature and precipitation in the context of a water management perspective rather than investigating energy exchanges. These estimates will be useful for long-term urban planning in terms of thermal exposure, water runoff drainage systems, and adaptation to counteract the effects of the urban heat island phenomenon.

2. Materials and Methods

2.1. Study Area and Datasets

Cyprus is an island in the eastern basin of the Mediterranean Sea with an area of 9251 km². Daily values of ambient temperature and precipitation were obtained from an urban station (35.17° N, 33.36° E) located in the city center and a suburban station (35.14° N, 33.40° E) in Nicosia for the years 1988 to 2017. Later, longwave radiation, UVA, UVB, cloud cover, and absolute humidity were also analyzed for the suburban meteorological station for the years 2007 to 2017. The datasets used during the current study were collected by the Meteorological Service of the Ministry of Agriculture, Rural Development, and Environment (MARDE) in the Republic of Cyprus.

2.2. DTR Index and Statistical Analysis

DTR is defined here (Equation 1) as the difference between the daily maximum ambient air temperature (MAXT) and daily minimum ambient air temperature (MINT) at each station. These three parameters—DTR, MAXT, and MINT—were investigated seasonally (December–February (DJF), March–May (MAM), June–August (JJA), and September–November (SON)).

$$DTR = MAXT - MINT \quad (1)$$

We estimated the p-values of the three parameters using the one-sided Student's test and set a false rejection rate of $p > 0.01$ to include only statistically significant data. The data appeared to have a skewness and kurtosis deviating a lot from zero signifying not normal distribution. The Mann–Kendall test was utilized for further analysis of DTR, MAXT, and MINT, as it is used to explore monotonic non-parametric trends in time-series data. This test was considered appropriate, since the dataset was periodically categorized. The Mann–Kendall statistic provides an indication of the existence of a trend and whether the trend is positive or negative, without being affected by extreme values or outliers. The Mann–Kendall statistic for the g^{th} season is calculated as:

$$S_g = \sum_{i=1}^{n-1} \sum_{j=i+1}^n \int x_{jg} - x_{ig} \quad (1 \leq g \leq m) \quad (2)$$

where $x_{jg} - x_{ig}$ is the difference between the later-measured value and all the earlier measured values where $j > i$, and with:

$$\int x = \begin{cases} 1 & \text{if } x > 0 \\ 0 & \text{if } x = 0 \\ -1 & \text{if } x < 0 \end{cases} \quad (3)$$

The seasonal Mann–Kendall statistic for the entire series is calculated according to:

$$\hat{S} = \sum_{g=1}^m S_g \quad (4)$$

where \hat{S} is the sum of the S from each season, S_g is the S from the g^{th} season, and m is the number of seasons.

2.3. Urbanization and Cluster Analysis for Local Climatic Parameters

Population varies spatially and temporally. Its spatiotemporal distribution is difficult to estimate because the demographic and socioeconomic characteristics of the population are only available through the census and were collected for the years 1981, 1991, 2001, and 2011. We showed the population growth and number of residences during the three decades, 1981–2011. The methodology suggested by Karl et al. [23] was utilized, which suggests calculation of the temperature differences between the urban and suburban pair of stations [23]. Later, we evaluated the t-test of the difference of

means (t values) between the urban and suburban stations for daily MAXT, MINT, and mean daily temperature (MEANT) denoting statistical significant difference for $p(t) < \alpha = 0.05$.

According to Table 1, the maximum temperatures (MAXT) were not significantly higher during the entire year in the urban station in relation to the suburban station. Nevertheless, comparing the minimum temperatures (MINT), the t-test values were statistically significant for all the months showing the large increase of minimum temperature in the suburban station over the 30 investigated years. The differences that were observed between the urban and suburban station on the mean daily temperatures, considering that this is not observed in the MAXT, is attributed to the upward heat release not being achieved sufficiently during the night due to the dense construction in the city center.

Table 1. T-test of the difference of means (t-values) between the urban and suburban stations for daily maximum ambient air temperature (MAXT), minimum ambient air temperature (MINT), and mean temperature (MEANT). The initials in the horizontal column indicate months of the year.

	J	F	M	A	M	J	J	A	S	O	N	D
MAXT	0.58	0.67	0.71	0.90	0.06	0.09	0.08	0.23	0.55	0.81	0.17	0.05
MINT	≈0	≈0	≈0	≈0	≈0	≈0	≈0	≈0	≈0	≈0	≈0	≈0
MEANT	≈0	≈0	≈0	≈0	≈0	≈0	≈0	≈0	≈0	0.07	0.56	≈0

After identifying a trend of MAXT, MINT, and DTR values over the 30 investigated years, the analysis of specific meteorological parameters of specific years was done in order to characterize the DTR variations based on the differences between them. The specific parameters were chosen based on the research of other studies that revealed a relationship with DTR, and the years were only chosen (years 2007, 2010, 2012, and 2014) based on the availability of complete meteorological data. The methodology used for the investigation of these meteorological parameters to characterize DTR was the K-means clustering algorithm.

The K-means clustering algorithm is a method that identifies unknown groups in complex data sets using iterative refinement. The K-means clustering method was used here to yield groups that represent frequently occurring weather patterns by computing the distances between the points and group centers of the parameters of the dataset, and then dividing the values into k cluster groups.

We performed a cluster analysis for the above-mentioned years for daytime and night-time values for the suburban station’s dataset. The meteorological parameters used to characterize each data point were DTR [°C], MAXT [°C], MINT [°C], downward longwave radiation [W/m²], upward longwave radiation [W/m²], net longwave radiation [W/m²], precipitation [mm], water vapor [kg/m³], and for daytime values, also UVA [W/m²], UVB [W/m²], and cloud cover [oktas].

Prior to the clustering analysis, we divided the dataset into two periods: a warm period (months May to October) and a cold period (months November to April) to minimize the effect of seasonal climatic effects on the results.

A preliminary cluster analysis of the datasets [24,25] showed the highly clusterable nature (close to 0) of the dataset with Hopkin statistical values of 0.12 (warm period) and 0.16 (cold period) for the daytime dataset and 0.11 (warm period) and 0.15 (cold period) for the night-time dataset. The Hopkin statistic is computed as 1-H:

$$H = \frac{\sum_{i=1}^m u_i^d}{\sum_{i=1}^m u_i^d + \sum_{i=1}^m w_i^d} \tag{5}$$

where u_i is the nearest neighbor distances from uniformly generated sample points to sample data from the given datasets, and w_i is the nearest neighbor distances within sample data from the given datasets.

The initial analysis also validated the datasets by determining the optimal number of clusters; three for both periods for daytime data, and three cluster groups for both periods for night-time data. Silhouette width analysis showed values of around 0.25 for daytime and night-time observations respectively, suggesting that the data are well clustered, but there is a small distance between each

cluster. The average distance within each cluster should be as small as possible, whereas the average distance between clusters should be as large as possible to obtain high silhouette widths coefficients (closer to one). In the results section, the cluster groups will be presented along with an explanation of the similar characteristics of each cluster group. The axis coordinates of the graphs represent principal components, which are linear combinations of the original dimensions, and describe the relations between parameters, and not absolute values.

3. Results

3.1. DTR Trend Analysis

A seasonal Mann–Kendall trend analysis was used to indicate the time-series trend when a cyclic trend (seasonal) occurs. Table 2 summarizes the results that evidence a decreasing DTR trend for the 30 investigated years (1988–2017) due to the larger increase of the minimum daily temperatures. The small p value (<0.01) shows that there is a monotonic trend, and the tau indicates whether this is an increasing or decreasing trend.

Table 2. Seasonal Mann–Kendall trends of daily maximum temperature (MAXT), minimum temperature (MINT), and diurnal air temperature range (DTR) per decade in Nicosia’s urban and suburban stations.

	Tau (τ)	2-Sided p -Value
Nicosia’s urban station		
MAXT	0.07	0.048
MINT	0.32	$<2.22e-16$
DTR	−0.24	$2.34e-10$
Nicosia’s suburban station		
MAXT	0.11	0.003
MINT	0.41	$<2.22e-16$
DTR	−0.36	$<2.22e-16$

The results show that a decreasing DTR of -0.24 °C/decade at the urban station and -0.36 °C/decade at the suburban station are both within the range of the earlier reported trends (varying from -0.14 °C/decade to -0.53 °C/decade) [22]. This shows the larger decreasing trend of DTR over the past 30 years compared to the previous century, and specifically the larger increasing trend of the minimum temperature. Therefore, in Section 3.2, urbanization was analyzed in terms of population growth and number of residences.

Figure 1 illustrates the trends of yearly seasonal diurnal air temperature range (DTR), maximum air temperature, and minimum air temperature for the years 1988–2017 for the urban and suburban stations in Nicosia. A clear decreasing trend of DTR (yellow line) was observed for the 30-year time period. In some time periods, the decrease was more noticeable, particularly during the decade 2000–2010. Both the maximum and minimum temperature demonstrated significant increasing trends, particularly in winter and autumn. In spring and summer, the minimum temperature appeared to have a higher increasing trend compared to the maximum temperature.

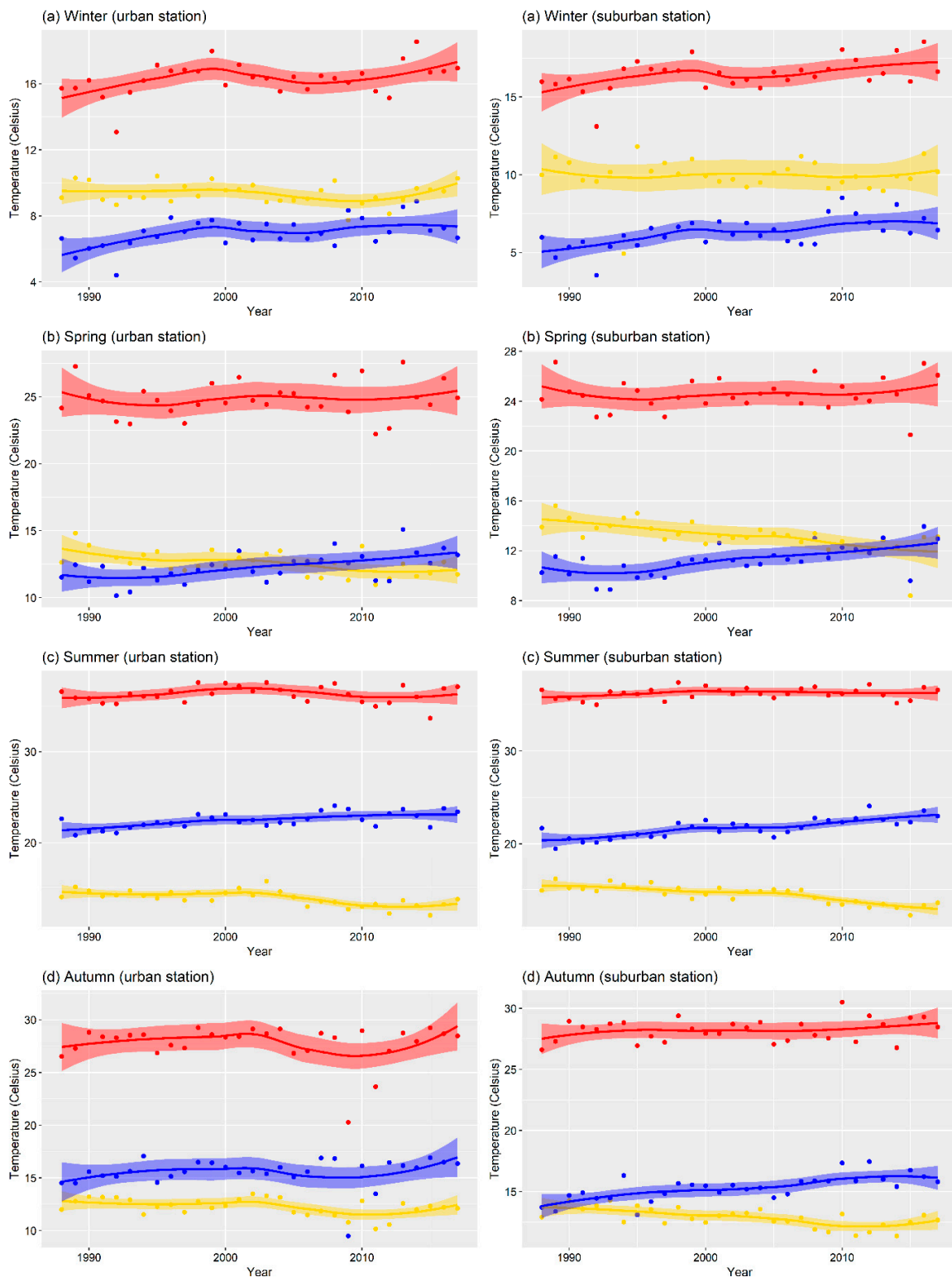


Figure 1. Mean seasonal value of DTR (yellow dots), daily maximum temperature (red dots), and daily minimum temperature (blue dots) along with the confidence intervals (95%) and loess line for the years 1988–2017 for Nicosia’s urban station (first column) and Nicosia’s suburban station (second column).

3.2. Urbanization

Land-use changes from urbanization, creating an urban heat island (UHI), may be partially responsible for the observed warming over land and the decreasing trend of DTR in the investigated

cities. The urbanization may transform a station from rural to suburban in a time span of decades resulting in the increased absorption of solar radiation, a decrease of evapotranspiration, and a release of anthropogenic heat, thereby resulting in a change of air temperatures, horizontal winds, and air quality. Zhou et al. [26] found a negative correlation of -0.77 between changes in DTR and changes in the percentage of urban population to the total population in China [26].

Figure 2 shows the location of the two investigated areas (figure 2). Investigating the population growth and number of residences in the areas surrounding the two investigated stations in Nicosia (unoccupied municipalities within radius of 2–3 km from the urban meteorological station and suburban meteorological station) revealed a significant increasing trend. Specifically, the population increased by 39% (from 110,460 to 153,384) and 84% (from 20,396 to 37,557) in the areas surrounding Nicosia's urban station and Nicosia's suburban station respectively over three decades (years 1981 to 2011). Moreover, the number of residences has doubled in a period of four decades in all the investigated areas evidencing the problem of urbanization and population growth leading to land-use changes. The number of residences increased by 104% (from 35,298 to 72,068) and 198% (from 5829 to 17,394) in Nicosia's urban station and Nicosia's suburban station, respectively.

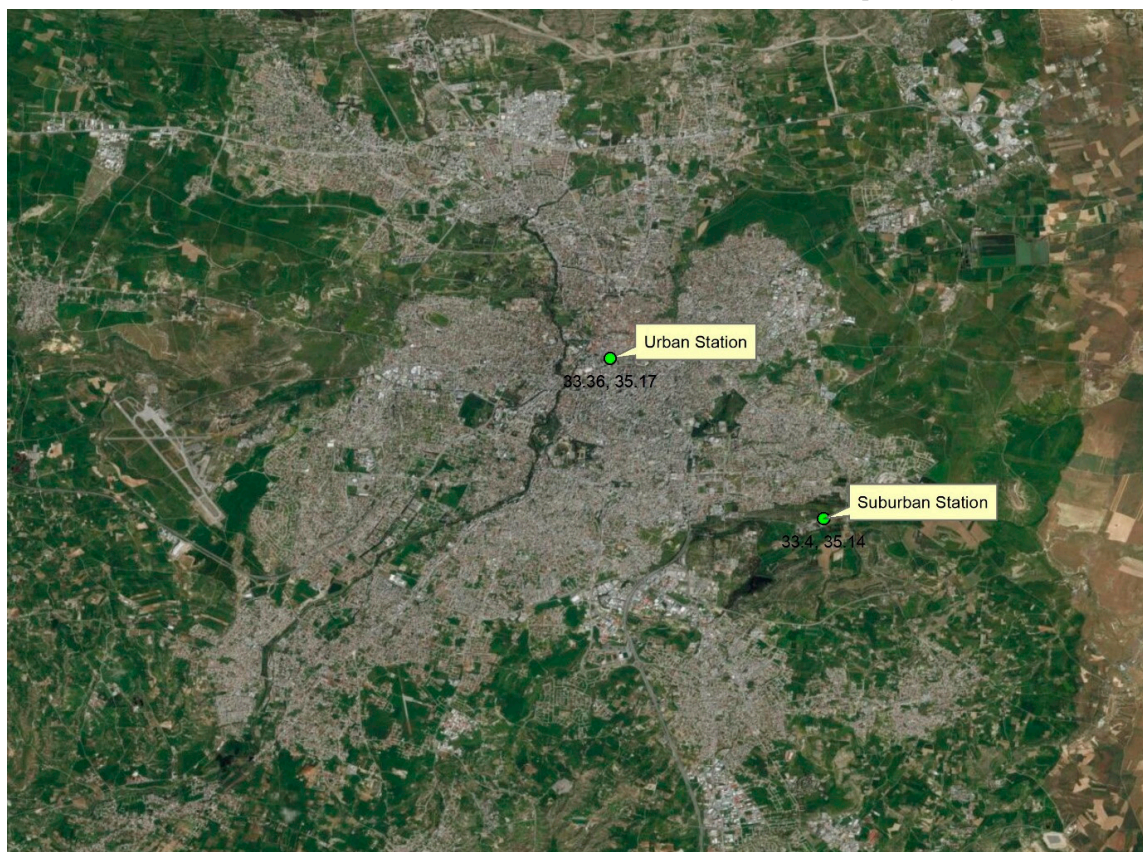


Figure 2. Map of Nicosia for year 2017 showing the location of the urban and suburban stations.

The large incline in population growth and number of residences resulted in an alternation in land use and urbanization, leading to increased temperatures and particularly minimum daily temperatures. In urban areas, the increased human activities and the lack of vegetation and surface moisture may amplify the impacts of urban development on surface temperatures and consequently air temperatures. Significant variations in DTR may be observed in different areas (urban, rural) due to differences in surface albedo, evapotranspiration, and longwave radiation. Zhou et al. [27] in their model suggested that a reduction of vegetation and soil emissivity/soil wetness may reduce the DTR by increasing the night-time surface air temperature during periods of drought [27]. Low emissivity reduces the

outgoing longwave radiation during night-time leading to temperature rise, especially over arid and semiarid regions.

3.3. Cluster Analysis for Regional Climatic Parameters

According to the seasonal Mann–Kendall test of Section 3.1, for the urban station, the minimum temperature had an increasing trend of 0.32 °C/decade, the maximum daily temperature had an increasing trend of 0.07 °C/decade, and the DTR had a decreasing trend of −0.24 °C/decade. A larger DTR was found in the summer, followed by spring, autumn, and finally winter. For the suburban station, the minimum and maximum temperatures had an increasing trend of 0.41 °C/decade and 0.11 °C/decade, respectively, and the DTR had a decreasing trend of −0.36 °C/decade.

In this section, we combined several parameters that were found in previous studies to explain the variations in DTR values. Further investigation was done for the years 2007, 2010, 2012, and 2014 using the following parameters from the suburban station for the identification of cluster groups: radiation (UVA, UVB, and longwave), precipitation, cloud cover, and absolute humidity data. The basic idea of the k-means clustering consists of defining clusters with low intra-cluster variation. The parameters on a day or night were considered as one observation that were assigned to a given cluster such that the sum of squares (SS) distance of the observation to the center of their assigned cluster would be minimized. A high total variance (SS between clusters divided by the total SS of all the clusters) is ideal, as it shows the percentage of values that were categorized into the created clusters with low intra-cluster variation.

Figure 3 shows the cluster analysis of night-time and daytime data, which investigated DTR, MINT, MAXT, precipitation, downward and upward longwave radiation, net longwave radiation, and water vapor. The water vapor values, downward, upward, and net longwave radiations corresponded to the time of the MAXT for daytime data clustering and of the MINT for night-time data clustering analysis. On the contrary, the average daily precipitation values were used for the clustering analysis. Table 3 shows the mean values of the parameters for each cluster for the night-time data, and Table 4 shows the mean values of the parameters for the daytime data.

Table 3. Mean values of investigated parameters for night-time data of the suburban station for the three clusters of each period.

Cluster	Cold period (NDJFMA)			Warm period (MJJASO)		
	1	2	3	1	2	3
DTR [°C]	11.3	13.2	9.1	13.6	11.9	13.5
Downward longwave [W/m ²]	248.0	286.2	285.8	351.4	305.9	321.7
Upward longwave [W/m ²]	314.5	353.7	340.2	427.3	366.8	396.5
Net longwave [W/m ²]	−66.5	−67.5	−54.5	−75.9	−60.9	−74.8
Precipitation [mm]	0.7	0.2	2.5	0.1	2.2	0.1
Water vapor [kg/m ³]	0.0071	0.0098	0.0084	0.018	0.012	0.013
Maximum temperature [°C]	16.6	25.2	18.5	37.3	27.3	32.2
Minimum temperature [°C]	5.3	12.0	9.4	23.7	15.4	18.7

For night-time data, cluster 3 had the smallest mean DTR compared to the other clusters in the same period. In summary, variations in DTR are mainly observed during the cold period. Particularly, high DTR based on the night-time data was observed at large net longwave radiation, low precipitation, and high water vapor. Low DTR based on the night-time data was observed for smaller net longwave radiation during the cold period.

Only eight parameters were used for the clustering of night-time data, which could explain about 65–70.7% of their total variance. For the daytime data, we used 11 parameters that explained 63.3–68.9% of the total variance; these values were lower than those for the night-time data, showing the importance of the existing parameters (temperature, downward and upward longwave radiation,

precipitation, and water vapor). A higher variance corresponds to a lower sum of the squared distances between data points and the center of their containing cluster. Specifically, the daytime data were divided into three clusters for the warm and cold period, as shown in Figure 3a,c. Table 4 shows the mean values of each parameters for the six clusters.

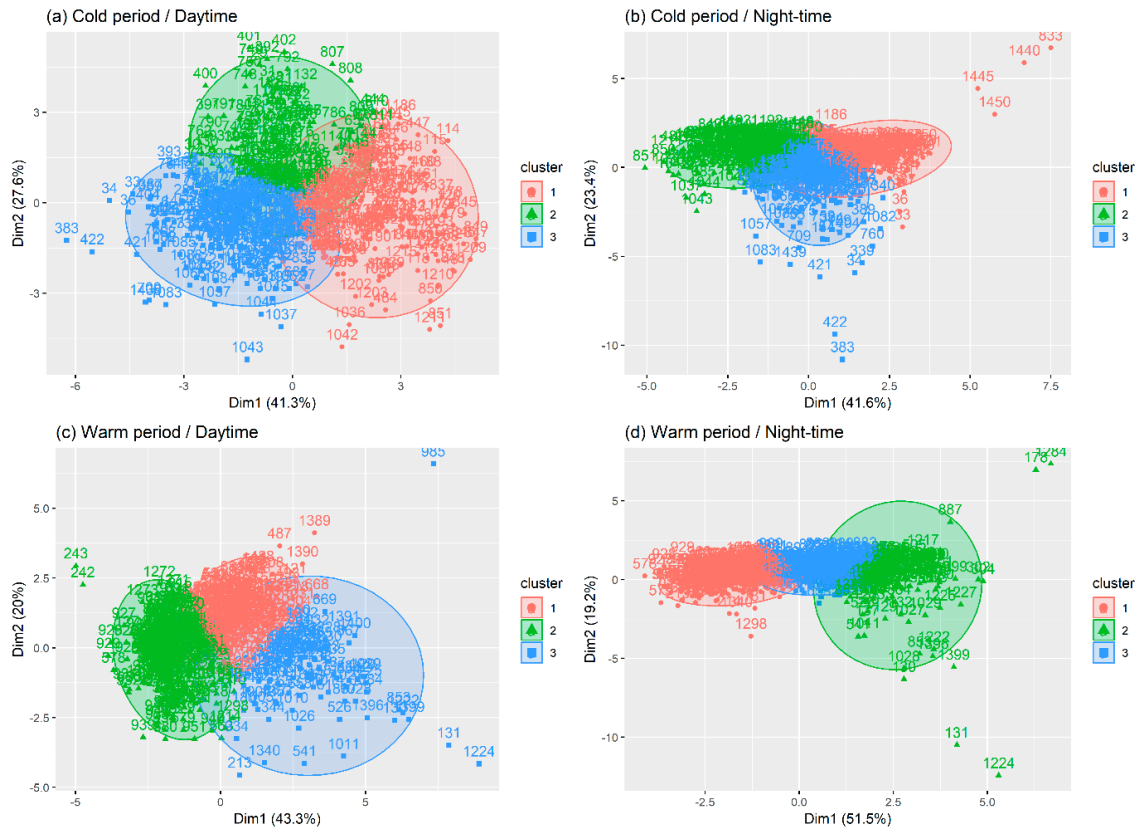


Figure 3. Cluster analysis of daytime and night-time data for the cold and warm periods at the suburban station.

Table 4. Mean values of investigated parameters for day-time data of the suburban station for the clusters of cold period (three clusters) and warm period (three clusters).

Cluster	Cold Period (NDJFMA)			Warm Period (MJJASO)		
	1	2	3	1	2	3
DTR [°C]	13.5	11.2	9.0	13.3	13.6	12.3
Downward longwave [W/m ²]	352.3	317.1	366.4	390.4	432.5	419.9
Upward longwave [W/m ²]	515.0	420.6	421.7	601.6	672.0	624.6
Net longwave [W/m ²]	−162.7	−103.5	−55.3	−211.2	−239.5	−204.7
Precipitation [mm]	0.0	0.17	3.1	0.01	0.08	1.3
Water vapor [kg/m ³]	0.0097	0.0077	0.010	0.013	0.017	0.016
Maximum temperature [°C]	24.7	16.8	18.0	30.6	37.1	33.7
Minimum temperature [°C]	11.2	5.5	9.0	17.2	23.5	21.3
UVA [W/m ²]	0.49	0.39	0.25	0.59	0.63	0.51
UVB [W/m ²]	0.03	0.02	0.01	0.05	0.05	0.04
Cloudiness [oktas]	3	3	6	3	2	3

According to Table 4, the lowest mean DTR was found for cluster number 3 with values of 9.0 °C and 12.3 °C for the cold and warm periods, respectively. Cluster 3 was also characterized by the smallest net longwave radiation (−55.3 W/m² cold period, −204.7 W/m² warm period), the lowest UVA and UVB, highest cloudiness (six oktas for the cold period, and three oktas for the warm

period)), frequent precipitation and with the lowest maximum and minimum temperatures among the three clusters.

On the contrary, clusters number 1 (cold period) and 2 (warm period) were characterized by a high DTR (13.5 °C and 13.6 °C) with the largest net longwave radiation (-162.7 W/m^2 cold period, -239.5 W/m^2 warm period), the highest UVA and UVB values, the lowest cloudiness and precipitation, and the highest water vapor and maximum and minimum temperatures.

We argue that high DTR is found at high net longwave radiation, during warm months without precipitation and with high UVA and UVB. Moreover, cloudiness and precipitation decrease DTR mainly by decreasing the maximum temperature, UVA, and UVB, and by increasing the highly negative net longwave radiation (due to lower upward radiation). Specifically, cloud droplets absorb and emit longwave radiation as a blackbody [28], but their radiative effects are largely affected by the surface albedo and solar zenith angle [29]. During clear days and days with few clouds, the DTR was larger, suggesting that more radiation reached the Earth's surface, resulting in higher temperatures during the day. On the contrary, on cloudy days (broken clouds or overcast), lower DTR values were calculated due to the lower daytime temperatures. High cloud cover reduces downward and upward longwave radiation, and the daytime temperature, MAXT, is lower. Dai et al. [13] also suggested that clouds mainly affect the daytime temperature by reducing the middle-day surface solar radiation. On the other hand, the night-time temperature decreases slightly because the downward longwave radiation differs only a little between cloudy and clear days [13].

Daily precipitation alone revealed a low relationship with DTR, but when combined with cloudiness and high absolute humidity, then it may be suggested that it has a more significant effect on DTR, agreeing with previous studies [13,14]. Under rainy conditions, the moisture content of the atmosphere and ground soil increases, leading to lower daytime temperatures due to evapotranspiration, but also higher night-time minimum temperatures due to the higher heat capacity of the water in wet soils. Enlarged DTR values are expected under dry conditions due to increased maximum temperatures and decreased minimum daily temperature [30]. Under wet conditions, the energy budget balance changes as the high soil moisture availability allows evaporative cooling, resulting in a further decrease in the temperatures.

Another parameter that was evaluated was water vapor/absolute humidity. Dry air (low water vapor) is associated with reduced cloudiness and therefore larger daytime solar radiation, which is UVA and UVB in this case. This is more apparent in the cold period. Even though more precipitation occurred in the winter/cold period, the highest absolute humidity was observed in the summer with values over 0.017 kg/m^3 . The large atmospheric moisture in the summer can make the downward longwave radiation less sensitive to the presence of low-level clouds, resulting in steadier downward longwave radiation values. Moreover, an increase in the absolute humidity in the atmosphere is a result of high incoming shortwave and longwave radiation in combination with limited water runoff that residues over impervious surfaces. With urban development, the natural surface runoff may completely disappear, and only human-made drainage systems are able to transport water out of the city. Inadequate drainage systems in the summer lead to evapotranspiration of overlay water upon impervious surfaces leading to higher absolute humidity, particularly in the summer when there is higher incoming radiation and evapotranspiration. Stenchikov and Robock [29] concluded that water vapor may reduce DTR due to its absorption of the solar radiation in the near infrared, and therefore resulting in lower maximum daily temperatures during the daytime [31]. Yeo et al. showed that during the winter, the downward longwave radiation depends on the cloud height as well as atmospheric temperature and humidity, whereas the upward longwave radiation is entirely dependent on the surface temperature [32].

The decreasing trend of DTR for the past 30 years may be explained primarily by the increase of the minimum daily temperature. From the clustering analysis of the meteorological data for the suburban station, it was shown that DTR is dependent and lower when precipitation occurs, when

there is higher net longwave radiation, low–medium water vapor, cloudiness over six oktas, and low minimum temperatures.

4. Discussion and Conclusions

Diurnal temperature range (DTR) appears to be a suitable index of climate variability because of the global climate change and UHI and change, especially in inland areas. This paper revealed a decreasing DTR trend in an inland town and its suburban area. The results in the previous section revealed a variable decreasing trend of DTR over the investigated years that was more notable in summer and spring. Specifically, there was a decreasing DTR of -0.24 °C/decade at the urban station and -0.36 °C/decade at the suburban station. This decreasing DTR trend over the investigated time period was due to larger increases of minimum daily temperatures than maximum daily temperatures. Higher minimum temperatures were observed on cloudy days because clouds emit longwave radiation downwards. The largest increases in nocturnal temperature through the years were attributed to the intense urbanization, as evidenced by the comparison of the temperatures of the urban–suburban pair of stations. The increase of impervious surfaces and excessive land use leads to variations of the heat fluxes throughout the day.

A factor that could affect the DTR decrease is the urbanization, resulting in the intensification of the urban heat island phenomenon. Urbanization reduces green space and increases impervious surfaces, and urban surfaces have lower albedo compared to rural surfaces [33]. Specifically, at night, the high urban constructions block outgoing radiation, and the advection of cool breeze from the rural areas reduces the rate of cooling. Moreover, anthropogenic heat released from human activities such as traffic and heating or cooling also contributes to the UHI and results in an increase of minimum daily temperatures. DTR's decreasing trend was higher in Nicosia's urban and suburban stations, where a higher population growth and larger number of residences was recorded compared to the rural station. Over a period of 40 years, the population within the Nicosia municipality increased from about 110,000 people to 154,000 people. The decrease of DTR was more noticeable in the suburban station, where the population increased by 84% in four decades in the surrounding area (Aglantzia and Latsia area).

Studies have sought to determine the controlling factors of DTR showing its reliance to clouds, soil moisture, precipitation, and radiation. As a preliminary step in understanding the causes of the decreasing DTR trend, we used the k-means clustering method to evaluate different meteorological parameters. Three clusters were found for night-time and daytime data for each investigated period. The total variance of the clusters was up to 70.7% and 68.9% for the night-time and daytime datasets. The limitations of this study were observed from the average percentage of variance of the clusters that could be further increased with the addition of other meteorological parameters that were not studied, such as wind speed and direction or atmospheric composition (sand blown from the nearby Middle East), which also affect cloud cover, absolute humidity, and longwave radiation. This addition may assist in the further understanding of the interaction of these meteorological variables. High DTR was found at low net longwave radiation during warm months without precipitation and with high UVA and UVB. Moreover, cloudiness and precipitation decrease DTR mainly by decreasing the maximum temperature, UVA, and UVB, and increasing the net longwave radiation. Daily precipitation was associated with DTR only for the night-time data during the cold period.

This study provides a coherent picture of the variability of several meteorological parameters that are strongly correlated with each other and were found in previous studies to affect the variations in DTR. Our results emphasize the need to focus on the unique aspects of urban climate to assess the effect of urbanization and anthropogenic sources in temperature increase, but also the development of a quantitative basis for assessing the DTR change.

Author Contributions: M.S. conceived the research topic. A.P. obtained the datasets, created the figures and analyzed the results. All authors (A.P., M.S. and I.L.) contributed in the discussion of the results and reviewed the manuscript.

Acknowledgments: The authors are grateful to the Ministry of Agriculture, Rural Development and Environment (MADRE) of the Republic of Cyprus for the Department of Meteorology historical meteorological data and the Ministry of Labour, Welfare and Social Insurance for the air quality data.

Conflicts of Interest: The authors declare no competing interests.

References

1. EUROSTAT Eurostat Database. Available online: <https://ec.europa.eu/eurostat/data/database> (accessed on 30 April 2019).
2. Akbari, H.; Cartalis, C.; Kolokotsa, D.; Muscio, A.; Pisello, A.L.; Rossi, F.; Santamouris, M.; Synnef, A.; Wong, N.H.; Zinzi, M. Local climate change and urban heat island mitigation techniques—The state of the art. *J. Civ. Eng. Manag.* **2015**. [[CrossRef](#)]
3. Santamouris, M. On the energy impact of urban heat island and global warming on buildings. *Energy Build.* **2014**, *82*, 100–113. [[CrossRef](#)]
4. Santamouris, M.; Cartalis, C.; Synnefa, A.; Kolokotsa, D. On the impact of urban heat island and global warming on the power demand and electricity consumption of buildings—A review. *Energy Build.* **2015**. [[CrossRef](#)]
5. Gasparrini, A.; Guo, Y.; Sera, F.; Vicedo-Cabrera, A.M.; Huber, V.; Tong, S.; de Sousa Zanotti Stagliorio Coelho, M.; Nascimento Saldiva, P.H.; Lavigne, E.; Matus Correa, P.; et al. Projections of temperature-related excess mortality under climate change scenarios. *Lancet Planet. Health* **2017**. [[CrossRef](#)]
6. Karl, T.R.; Jones, P.D.; Knight, R.W.; Kukla, G.; Plummer, N.; Razuvayev, V.N.; Gallo, K.P.; Lindesay, J.A.; Charlson, R.J.; Peterson, T.C. Asymmetric trends of daily maximum and minimum temperature: Empirical evidence and possible causes. *Bull. Am. Meteorol. Soc.* **1993**, *74*, 1007–1023. [[CrossRef](#)]
7. Braganza, K.; Karoly, D.J.; Arblaster, J.M. Diurnal temperature range as an index of global climate change during the twentieth century. *Geophys. Res. Lett.* **2004**, *31*, 2–5. [[CrossRef](#)]
8. New, M.; Hulme, M.; Jones, P. Representing twentieth-century space-time climate variability. Part II: Development of 1901–96 monthly grids of terrestrial surface climate. *J. Clim.* **2000**. [[CrossRef](#)]
9. Easterling, D.R.; Horton, B.; Jones, P.D.; Peterson, T.C.; Karl, T.R.; Parker, D.E.; Salinger, M.J.; Razuvayev, V.; Plummer, N.; Jamason, P.; et al. Maximum and minimum temperature trends for the globe. *Science* **1997**. [[CrossRef](#)]
10. Gallo, K.P.; Owen, T.W.; Easterling, D.R.; Jamason, P.F. Temperature trends of the U.S. historical climatology network based on satellite-designated land use/land cover. *J. Clim.* **1999**, *12*, 1344–1348. [[CrossRef](#)]
11. Wang, K.; Ye, H.; Chen, F.; Xiong, Y.; Wang, C. Urbanization effect on the diurnal temperature range: Different roles under solar dimming and brightening. *J. Clim.* **2012**, *25*, 1022–1027. [[CrossRef](#)]
12. Kueh, M.T.; Lin, C.Y.; Chuang, Y.J.; Sheng, Y.F.; Chien, Y.Y. Climate variability of heat waves and their associated diurnal temperature range variations in Taiwan. *Environ. Res. Lett.* **2017**, *12*. [[CrossRef](#)]
13. Dai, A.; Trenberth, K.E.; Karl, T.R. Effects of clouds, soil moisture, precipitation, and water vapor on diurnal temperature range. *J. Clim.* **1999**. [[CrossRef](#)]
14. Zhou, L.; Dai, A.; Dai, Y.; Vose, R.S.; Zou, C.Z.; Tian, Y.; Chen, H. Spatial dependence of diurnal temperature range trends on precipitation from 1950 to 2004. *Clim. Dyn.* **2009**. [[CrossRef](#)]
15. Pastor, F.; Valiente, J.A.; Palau, J.L. Sea Surface Temperature in the Mediterranean: Trends and Spatial Patterns (1982–2016). *Pure Appl. Geophys.* **2017**. [[CrossRef](#)]
16. Nykjaer, L. Mediterranean Sea surface warming 1985–2006. *Clim. Res.* **2009**. [[CrossRef](#)]
17. Shaltout, M.; Omstedt, A. Recent sea surface temperature trends and future scenarios for the Mediterranean Sea. *Oceanologia* **2014**. [[CrossRef](#)]
18. Founda, D.; Pierros, F.; Petrakis, M.; Zerefos, C. Interdecadal variations and trends of the Urban Heat Island in Athens (Greece) and its response to heat waves. *Atmos. Res.* **2015**, *161*, 1–13. [[CrossRef](#)]
19. Sun, X.; Ren, G.; You, Q.; Ren, Y.; Xu, W.; Xue, X.; Zhan, Y.; Zhang, S.; Zhang, P. Global diurnal temperature range (DTR) changes since 1901. *Clim. Dyn.* **2018**. [[CrossRef](#)]
20. Whan, K.; Zscheischler, J.; Orth, R.; Shongwe, M.; Rahimi, M.; Asare, E.O.; Seneviratne, S.I. Impact of soil moisture on extreme maximum temperatures in Europe. *Weather Clim. Extrem.* **2015**, *9*, 57–67. [[CrossRef](#)]
21. Bilbao, J.; Roman, R.; de Miguel, A. Temporal and Spatial Variability in Surface Air Temperature and Diurnal Temperature Range in Spain over the Period 1950–2011. *Climate* **2019**, *7*. [[CrossRef](#)]

22. Price, C.; Michaelides, S.; Pashiardis, S.; Alpert, P. Long term changes in diurnal temperature range in Cyprus. *Atmos. Res.* **1999**, *51*, 85–98. [[CrossRef](#)]
23. Karl, T.R.; Diaz, H.F.; Kukla, G. Urbanization: Its Detection and Effect in the United States Climate Record. *J. Clim.* **2002**. [[CrossRef](#)]
24. Maechler, M.; Rousseeuw, P.; Struyf, A.; Hubert, M.; Hornik, K.; Studer, M.; Roudier, P.; Gonzalez, J. Cluster: ‘Finding Groups in Data’: Cluster Analysis Extended Rousseeuw et Al. (version 2.0.6). 2017. Available online: <http://cran.us.r-project.org/web/packages/cluster/index.html>.
25. Kassambara, A.; Mundt, F. factoextra: Extract and Visualize the Results of Multivariate Data Analyses. <https://CRAN.R-project.org/package=factoextra>, R package version 1.0.3, 2016.
26. Zhou, L.; Dickinson, R.E.; Tian, Y.; Fang, J.; Li, Q.; Kaufmann, R.K.; Tucker, C.J.; Myneni, R.B. Evidence for a significant urbanization effect on climate in China. *Proc. Natl. Acad. Sci. USA* **2004**, *101*, 9540–9544. [[CrossRef](#)] [[PubMed](#)]
27. Zhou, L.; Dickinson, R.E.; Tian, Y.; Vose, R.S.; Dai, Y. Impact of vegetation removal and soil aridation on diurnal temperature range in a semiarid region: Application to the Sahel. *Proc. Natl. Acad. Sci. USA* **2007**, *104*, 17937–17942. [[CrossRef](#)] [[PubMed](#)]
28. Schneider, G.; Paluzzi, P.; Oliver, J.P. Systematic Error in the Synoptic Sky Cover Record of the South Pole. *J. Clim.* **2002**. [[CrossRef](#)]
29. Shupe, M.D.; Intrieri, J.M. Cloud radiative forcing of the Arctic surface: The influence of cloud properties, surface albedo, and solar zenith angle. *J. Clim.* **2004**. [[CrossRef](#)]
30. He, B.; Huang, L.; Wang, Q. Precipitation deficits increase high diurnal temperature range extremes. *Sci. Rep.* **2015**, *5*, 12004. [[CrossRef](#)] [[PubMed](#)]
31. Stenchikov, G.L.; Robock, A. Diurnal asymmetry of climatic response to increased CO₂ and aerosols: Forcings and feedbacks. *J. Geophys. Res. Atmos.* **1995**, *100*, 26211–26227. [[CrossRef](#)]
32. Yeo, H.; Park, S.J.; Kim, B.M.; Shiobara, M.; Kim, S.W.; Kwon, H.; Kim, J.H.; Jeong, J.H.; Park, S.S.; Choi, T. The observed relationship of cloud to surface longwave radiation and air temperature at Ny-Ålesund, Svalbard. *Tellus B Chem. Phys. Meteorol.* **2018**, *70*, 1–10. [[CrossRef](#)]
33. Oke, T.R. The energetic basis of the urban heat island. *Q. J. R. Meteorol. Soc.* **1982**. [[CrossRef](#)]



© 2019 by the authors. Licensee MDPI, Basel, Switzerland. This article is an open access article distributed under the terms and conditions of the Creative Commons Attribution (CC BY) license (<http://creativecommons.org/licenses/by/4.0/>).